JOURNAL OF Materials CHEMISTRY

Stability and electronic property investigations of the graphitic C_3N_4 system showing an orthorhombic unit cell

Maurizio Mattesini,* Samir F. Matar and Jean Etourneau

Institut de Chimie de la Matière Condensée de Bordeaux, I.C.M.C.B-CNRS, 87, Avenue du Dr. Albert Schweitzer, F-33608 Pessac Cedex, France.
E-mail: mattesim@icmcb.u-bordeaux.fr

Received 9th November 1999, Accepted 20th December 1999

Recently, Alves *et al.* have suggested a new orthorhombic lattice system as a possible form for the graphitic C_3N_4 model structure. For this new phase, some modifications in the electronic properties are expected with respect to the hexagonal variety previously proposed by Teter and Hemley. A theoretical investigation of the stability and electronic properties has been carried out in this work for the orthorhombic phase. The crystal geometry was relaxed using an ultrasoft pseudopotential method. The electron density map and density of states were calculated successively with a full-potential linearized augmented plane-wave code. The orthorhombic system shows a marked snake-like electron density path along the *b* crystallographic axis, bringing about more metallic behaviour in the solid. As a consequence, disappearance of the band gap occurs on going from the hexagonal to the orthorhombic lattice system. Special attention has also been devoted to the description of the chemical bonding in the graphitic C_3N_4 layer. The augmented spherical wave method has been employed to carry out crystal orbital overlap population analyses of the hexagonal and orthorhombic phases.

1 Introduction

The synthesis of super-hard materials of the C_3N_4 type is still restricted to the production of small amounts which are not sufficient for adequate structural characterisation. Experimentalists have observed that carbon nitride materials exist in amorphous or disordered phases,[1–3] as well as a crystalline phase dispersed in the amorphous matrix.[4,5] This restriction is possibly due to the technological difficulties associated with production of materials containing the large amounts of nitrogen which are required to chemically interact with carbon.

Theoretical publications on the subject have attempted to explain the stability and mechanical properties of some of the synthesised crystalline carbon nitrides and to predict the properties of the new hypothetical forms.[6–13] Several theoretical structures have been suggested for carbon nitride with super-hard behaviour, these being β-C_3N_4[9,12,14,15] and α-C_3N_4[12] (formally derived from α- and β-Si_3N_4), pseudo-cubic (structure derived from α-$CdIn_2Se_4$) and cubic (deduced from the high pressure form of Zn_2SiO_4). A graphitic structure has also been considered as one of the possible forms for the carbon nitride.[10,12,16] In order to obtain the graphitic form of C_3N_4, two carbon atoms must be replaced with a single nitrogen, with consequent creation of a carbon vacancy. In the Teter and Hemley model[12] the vacancies are ordered in such a way that a hexagonal unit cell results (Fig. 1). Different stacking-ordering types were proposed, leading to a rhombohedral lattice.[9,10] All these phases are based on the same order for the vacancies. Recently, Alves *et al.*[17] have introduced a new order for the carbon vacancies which leads to an orthorhombic lattice (Fig. 2). In this new phase, a different bonding conjugation is expected due to the participation of the N_1 nitrogen in the π-delocalisation along the *b*-axis. The double coordination of the N_1 atom present in the orthorhombic phase allows a connection between the double bond resonances present in the adjacent C_3N_3 rings, thus offering the possibility for electron delocalisation along the graphitic layer. Conversely, the hexagonal phase shows a three-coordinated N_1 atom which hinders expansion of the electron delocalisation along the graphitic layer. In short, the hexagonal lattice shows a localised electronic resonance inside each C_3N_3 ring while in the orthorhombic version, extended electron delocalisation is found along the *b*-axis.

From this, the purpose of this article is to examine the stability and the electronic properties of the orthorhombic lattice with respect to the hexagonal phase in order to present a theoretical justification for the existence of a reasonable new C_3N_4 graphitic model. By using the pseudopotential (PP) and plane-wave (PW) basis set approach and the full-potential linearized augmented plane-wave (FP-LAPW) method, differences in stability and electronic behaviour between the hexagonal and orthorhombic lattices are highlighted. For simplicity, the AAA stacking mode has been considered for both lattice types. Further, the augmented spherical wave (ASW) method has been applied to describe the hybridisation influence on the chemical bonding inside the graphitic layer: the crystal orbital overlap population (COOP) analysis is presented.

2 Computational details

Our calculations were carried out in the frame of density functional theory (DFT) within the finite-temperature local density approximation (LDA)[18,19] to the electron exchange and correlation (VASP package[19–22]). The interactions between the ions and the electrons are described using the ultrasoft Vanderbilt pseudopotential (US-PP)[23] and the electron–electron interaction is treated within the LDA by the Ceperley–Alder exchange-correlation potential.[24] In the plane-wave pseudopotential approach, rapid variation of the potential near the nuclei is avoided by substituting the Hamiltonian near the atoms with a smoother pseudo-Hamiltonian which reproduces the valence energy spectrum. The core states are removed with rapid variations of the wavefunctions near the nucleus. The PP allows a considerable reduction of the necessary number of plane-waves per atom for transition metal and first row elements, thus force and full

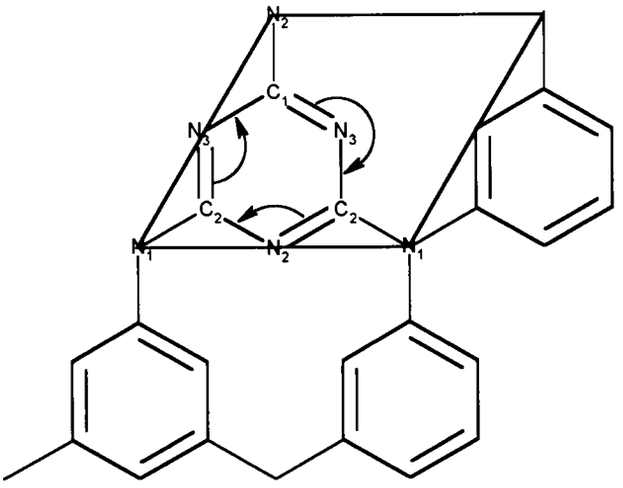

Fig. 1 Hexagonal unit cell of C_3N_4.

stress tensors can be easily calculated and used to relax atoms into their ground state.

A complete ion and volume relaxation was performed for the orthorhombic phase using the conjugate-gradient algorithm[25] and an energy cut-off of 25.57 Ry (1 Ry = 13.605698 eV) for the plane-wave basis set. The Methfessel–Paxton smearing scheme[26] was used for geometry relaxation, while the tetrahedron method with Blöchl corrections[27] was implied for the total energy calculations. A k-point sampling using a $10 \times 10 \times 10$ Monkhorst–Pack grid[28] was used throughout all the calculations performed in this work.

Total energy calculations and electron density maps were performed on the optimised structure using accurate full potential total energy calculations (WIEN97 package[29]). The number of plane-waves per atom used was 172 and a total of 100 k-points were implied, with a $4 \times 4 \times 4$ sampling. For carbon and nitrogen atom types the same muffin-tin radius ($R_{MT} = 1.33$ Å) was used.

A qualitative stabilisation feature was assessed using the chemical bonding criteria. The COOPs were evaluated for the two C_3N_4 systems by using the ASW method.[30] Calculations were performed by applying the tetrahedron method for the k-space integration and 217 irreducible k-points (energy converging with k-points, $\Delta E < 10^{-6}$ Ry) generated from a uniform $12 \times 12 \times 12$ mesh according to the Monkhorst–Pack scheme. Besides the LDA, the ASW method uses the atomic sphere approximation (ASA), in which each atom is represented by a sphere; the total volume of all the spheres is equal to the cell volume. Within the ASA, one usually has to introduce pseudoatoms ($Z = 0$) or empty spheres in order to ensure continuous electronic density in open structures. In the present calculations, we paid particular attention to optimising the choice of atomic radii as well as to the number and position of empty spheres used to meet the ASA criteria.

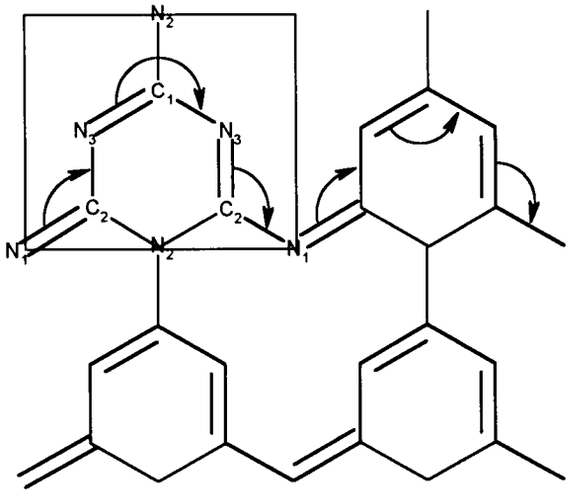

Fig. 2 Orthorhombic unit cell of C_3N_4.

3 Structures and geometry optimisation

The geometry of the orthorhombic phase (Fig. 3) was taken from the original work of Alves *et al.*[17] and for simplicity the AAA stacking order was considered. This phase consists of 7 atoms per unit cell and belongs to the *P2mm* space group. As can be clearly seen from Fig. 3, a different vacancy ordering

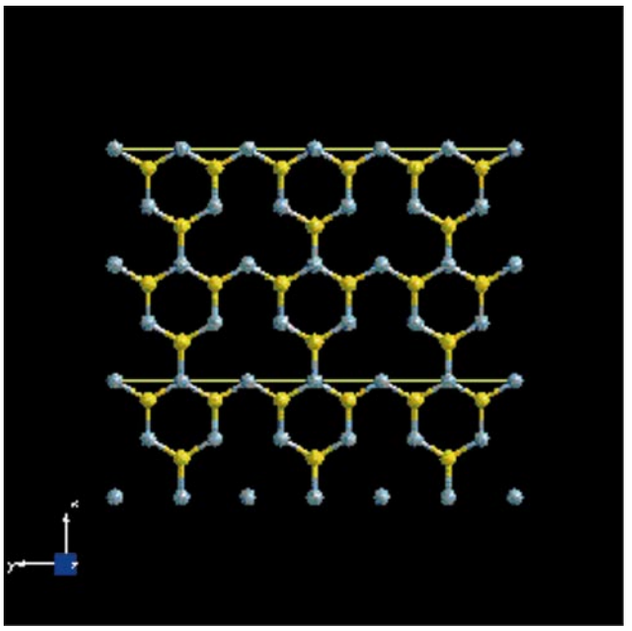

Fig. 3 Orthorhombic graphitic C_3N_4 proposed by Alves *et al.* A different vacancy ordering inside the graphitic plane is found. Nitrogen and carbon atoms are depicted in blue and yellow, respectively. This colour scheme is kept throughout this paper.

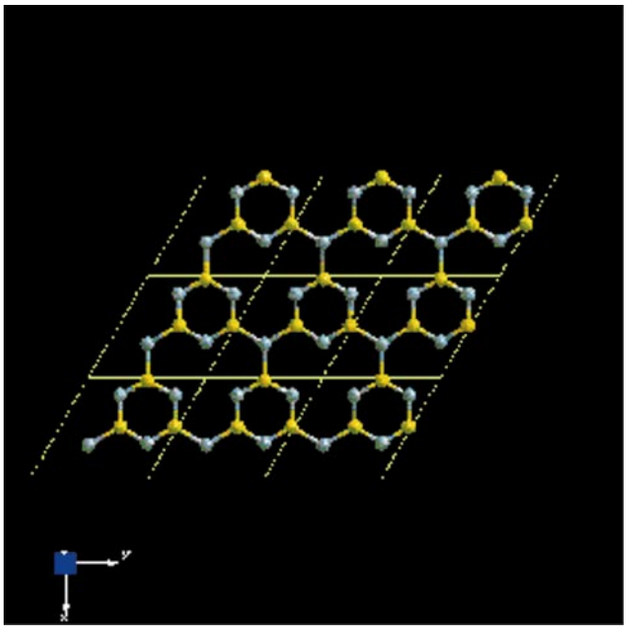

Fig. 4 Hexagonal unit cell proposed by Teter and Hemley.[12]

Table 1 Structural parameters for the orthorhombic structure with AAA stacking order

	Starting geometry from Alves *et al.*[17]	Optimised structure from the US-PP method
Space group	*P2mm*	*P2mm*
Parameters/Å	$a=4.1$, $b=4.7$, $c=3.2$	$a=4.11973$, $b=4.71049$, $c=3.12329$
Atomic positions	N1 (1a) (0.000, 0.000, 0.000)	N1 (−0.021, 0.000, 0.000)
	N2 (1c) (0.000, 0.500, 0.000)	N2 (0.009, 0.500, 0.000)
	N3 (2e) (0.500, 0.250, 0.000)	N3 (0.505, 0.258, 0.000)
	C1 (1c) (0.333, 0.500, 0.000)	C1 (0.351, 0.500, 0.000)
	C2 (2e) (0.833, 0.750, 0.000)	C2 (0.824, 0.757, 0.000)

inside the graphitic plane is present with respect to the hexagonal model proposed by Teter and Hemley[12] (Fig. 4). The hexagonal unit cell contains 7 atoms and the symmetry is $P\bar{6}m2$.[10,12]

In both unit cells, each C atom is three-fold coordinated, as is one of the four N atoms per cell, while the other three N atoms are two-fold coordinated. From this different vacancy ordering, a modification in the electronic properties is expected in the orthorhombic phase with respect to the hexagonal form due to the an increased electronic participation of the N_1 nitrogen in the C_3N_3 heterocycle.

Starting from the geometry given by Alves *et al.*, the orthorhombic structure was optimised using the PP method. Table 1 shows the structural parameters relative to the orthorhombic phase before and after the full geometry optimisation. The most important modification found in the optimised structure is the change in the geometry relative to the C_3N_3 heterocycle. These rings are now less symmetric than they were before the structural relaxation. A shortening in the interlayer distance from 3.20 to 3.12 Å is also found in the optimised geometry. A brief summary of the most important geometry changes in the orthorhombic phase is shown in Table 2. The atomic labelling schemes are given in Fig. 1 and 2. It is important to note that optimisation of the hexagonal phase under the same conditions still leads to a symmetric geometry for the C_3N_3 rings.

4 Relative stability between the two graphitic phases

The FP-LAPW method predicts a stability for the new orthorhombic structure comparable to that shown by the hexagonal phase. Table 3 gives the calculated total energy values for the orthorhombic and hexagonal structures. Although the energy reference is not the same for the two methods (core states are not included in the PP calculations), the energy differences between the two forms show values of a similar order of magnitude, in favour of the orthorhombic variety: $\Delta E=0.0038$ eV (FP-LAPW calculations) and $\Delta E=0.0021$ eV (US-PP calculations). These results confirm that the existence of the orthorhombic phase as a reasonable structure for the C_3N_4 graphitic form is a possibility, as already mentioned in ref. 17.

Table 3 FP-LAPW and US-PP total energy calculations for the orthorhombic and hexagonal lattices

	Total energies/eV	
Structure	FP-LAPW	US-PP
Hexagonal	−9003.622351	−64.830090
Orthorhombic	−9003.626151	−64.832190
$\lvert\Delta E\rvert$	0.0038	0.0021

The stability difference can also be qualitatively discussed by weighting the DOS with the sign and magnitude of the overlap integral between the orbitals of atoms of different sorts; a comprehensive account from the chemistry standpoint was given by Hoffman.[31] The COOPs are positive when they describe bonding states and negative when they describe antibonding states; non-bonding states should exhibit COOPs of very low intensity. In this article, a qualitative description of the chemical bond is given with the recently implemented COOP in the ASW program.[30]

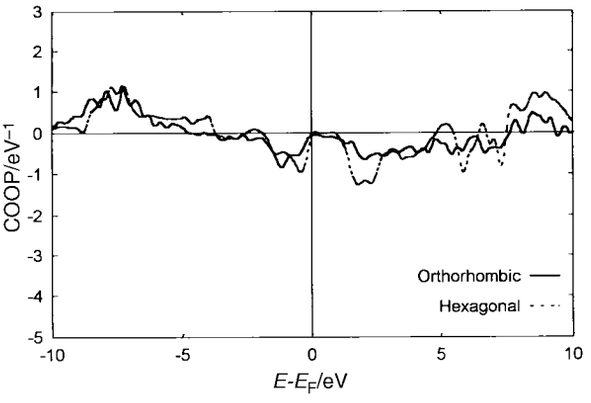

Fig. 5 Total COOPs for the hexagonal and orthorhombic phase (ASW).

Table 2 Intralayer geometry before and after the optimisation of the orthorhombic structure. The atoms carrying the prime notation belong to the adjacent unit cell

	Starting geometry from Alves *et al.*[17]	Optimised structure from the US-PP method
Bond lengths/Å	$d(N_1–C_2)=1.359$	$d(N_1–C_2)=1.311$
	$d(C_2–N_2)=1.359$	$d(C_2–N_2)=1.431$
	$d(C_2–N_3)=1.365$	$d(C_2–N_3)=1.316$
	$d(C_1–N_3)=1.359$	$d(C_1–N_3)=1.305$
	$d(N_2–C_1)=1.365$	$d(N_2–C_1)=1.409$
Angles/°	$N_1–C_2–N_3=120.23$	$N_1–C_2–N_3=122.23$
	$N_1–C_2–N_2=119.54$	$N_1–C_2–N_2=118.65$
	$N_3–C_2–N_2=120.23$	$N_3–C_2–N_2=119.12$
	$C_2–N_3–C_1=120.23$	$C_2–N_3–C_1=122.18$
	$N_3–C_1–N_3=119.54$	$N_3–C_1–N_3=121.80$
	$C_2–N_2–C_2=119.54$	$C_2–N_2–C_2=115.62$
	$C_2–N_1–C_2'=119.54$	$C_2–N_1–C_2'=121.69$
	$C_2–N_2–C_1'=120.23$	$C_2–N_2–C_1'=122.19$

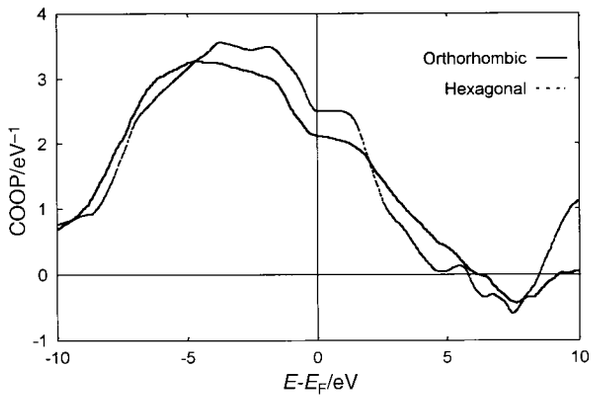

Fig. 6 Integrated COOPs for hexagonal and orthorhombic lattice system (ASW).

The total and integrated COOPs for the hexagonal and orthorhombic phases are shown in Fig. 5 and 6, respectively. The stability of the two phases appears almost the same; in the lower energy region of the valence band (VB) the two curves are mainly of bonding character (s states), while at energies closer to the Fermi level (E_F) the antibonding states of the p orbitals start to dominate. The antibonding counterparts are found in the conduction band (CB) centred at around 2 and 7 eV, while bonding behaviour appears at higher energy. Due to the larger electron delocalisation present in the orthorhombic lattice, the COOP is smeared out in comparison to the hexagonal system.

If the total COOP is projected into the corresponding contributions arising from the different atoms (Fig. 7), it can clearly be seen that in the lower region of the VB the N_3–C_1 interaction determines the positive contribution to the COOP, even if all the other carbon–nitrogen interactions are showing bonding character. At an energy close the E_F, the main bonding character is found for the N_3–C_1 and N_1–C_2 interactions while N_2–C_2 shows nearly non-bonding behaviour, and C_2–N_3 a negative COOP. This description of the bonding within the layer seems to favour the snake-like delocalisation in as far as the C_2–N_3 interaction is close to non-bonding. However, not all the interactions along the chain seem to behave as strongly bonding as N_3–C_1, for instance, the C_2–N_3 interaction is responsible for the antibonding behaviour below E_F. This shows the difficulty of carrying out this analysis to the point of making it resemble the picture expected by a chemist in his view of the resonant bonds. This restriction is mainly due to the fact that our COOP analysis does not use a directional orbital approach, since all contributions from p_x, p_y and p_z are included.

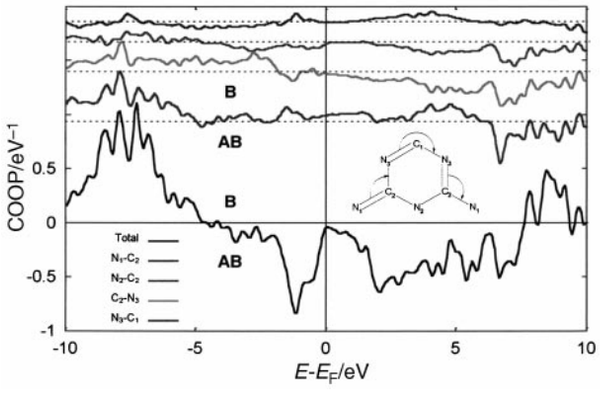

Fig. 7 Total COOP for the orthorhombic phase (ASW). For clarity each nitrogen–carbon interaction has been shifted along the vertical axis. The labels B and AB define the bonding and the antibonding regions, respectively.

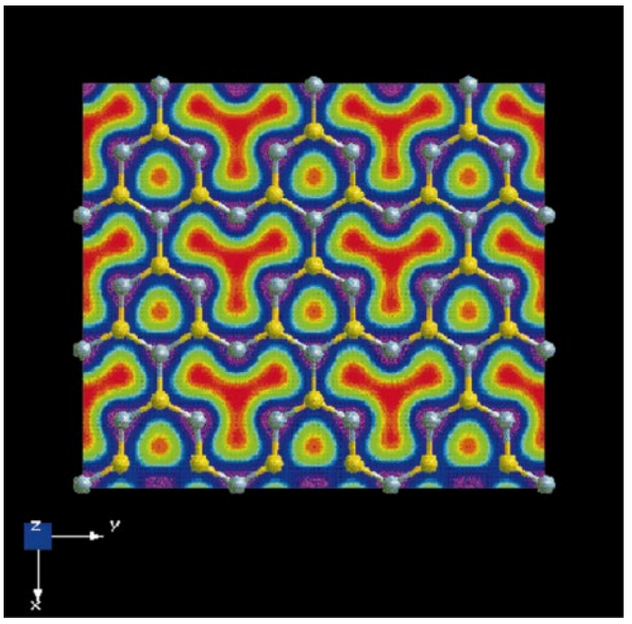

Fig. 8 Valence electron density map (FP-LAPW) for the optimised orthorhombic structure. The electronic density increases on going from the red to the violet isolines. This figure has been obtained using the XCrySDen graphical user interface.[32]

5 Electronic properties

By looking at the electronic density maps calculated within the FP-LAPW method for the orthorhombic phase, we can clearly see a charge density delocalisation (refer to the violet isolines) along the direction of the *b*-axis with a snake-like shape (Fig. 8). This new geometry seems to heavily influence the electronic properties of the orthorhombic structure giving a density of states without a band gap. The total DOS plot (FP-LAPW method) relative to the orthorhombic phase (Fig. 9) with the AAA stacking mode proposed by Alves *et al.*, clearly shows that a greater degree of metallic behaviour is present in this new graphitic form; the electronic levels of the nitrogen and carbon atoms now cross the E_F. This behaviour confirms the previous hypothesis of Alves *et al.* concerning a modification of the electronic structure due to the stronger role played by N_1 in mediating between neighbouring heterocycles.

For the hexagonal graphitic C_3N_4 system, the calculated electronic density map (Fig. 10) shows confined electronic circulation (violet isolines) inside the C_3N_3 rings. A band gap of 1.48 eV is found in the total DOS analysis performed with the FP-LAPW approach (Fig. 11).

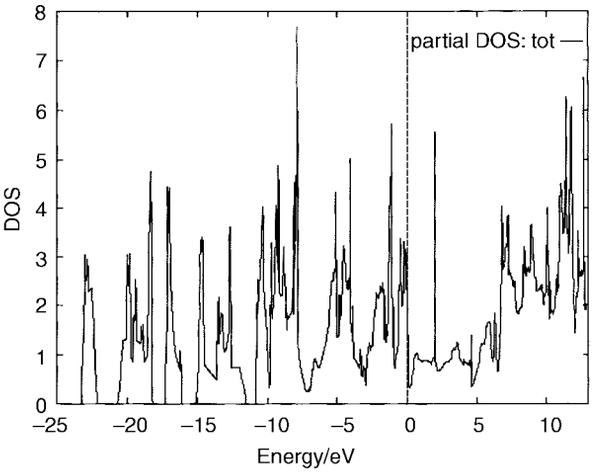

Fig. 9 Total DOS for the orthorhombic phase (FP-LAPW).

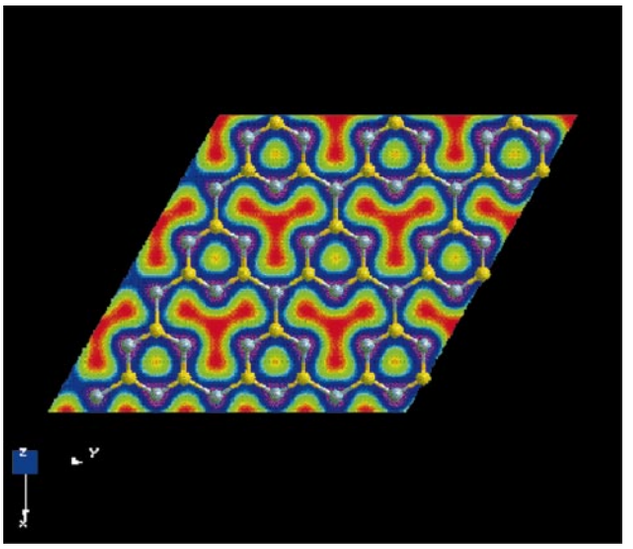

Fig. 10 Valence electron density map (FP-LAPW) for the optimised hexagonal structure. The electronic density increases on going from the red to the violet isolines (XCrySDen).

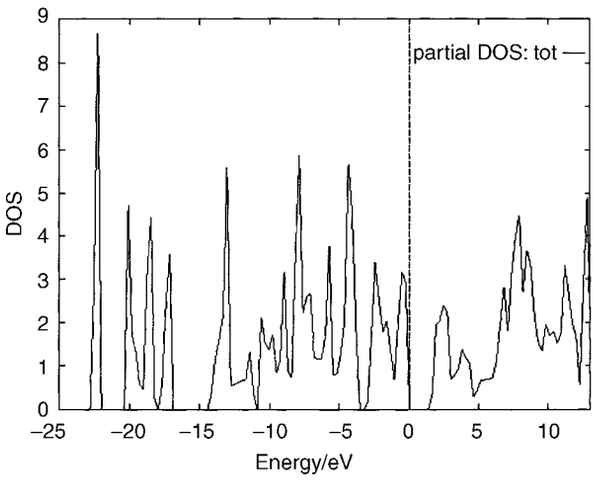

Fig. 11 Total DOS for the hexagonal phase (FP-LAPW).

6 Concluding remarks

The optimisation of the orthorhombic phase with the US-PP leads to an asymmetric equilibrium structure for the C_3N_3 ring inside the graphitic C_3N_4 layer. A shortening of the carbon–nitrogen bonds is found along the snake-like path due to the π-delocalisation present in the direction of the *b*-axis. The electron density map calculated with the FP-LAPW method also confirms the possibility for the orthorhombic phase to extend the electron delocalisation between the adjacent C_3N_3 rings. This behaviour is mainly due to the change in the coordination number for the N_1 atom, which goes from a three-fold coordination in the hexagonal lattice to a two-fold coordination in the orthorhombic state.

From a DOS analysis performed with the FP-LAPW method a greater degree of metallic behaviour was found for the orthorhombic system; the electronic states now cross the E_F and the band gap disappears.

Furthermore, the FP-LAPW and US-PP methods agree quite well in predicting a small energy difference between the two phases. From the COOP analysis, a qualitative estimation of the relative stability was also found to be in agreement with the two methods previously mentioned. Both lattice systems seem to be reasonable proposals for the graphitic C_3N_4 model, even though a clear change in the electronic properties was found for the orthorhombic phase.

Acknowledgements

This work was financially supported by the Training and Mobility of Researchers (TMR) Network: *Synthesis, structure and properties of new carbon-based hard materials* (FMRX-CT97-0103).

References

1 A. R. Merchant, D. G. McCulloch, D. R. McKenzie, Y. Yin, L. Hall and E. G. Gerstner, *J. Appl. Phys.*, 1988, **79**, 6914.
2 M. Y. Ching, D. Li, X. Lin, V. P. Dravid, Y. Chung, M. Wong and W. D. Sproul, *J. Vac. Sci. Technol., A*, 1993, **11**, 521.
3 D. M. Bhusari, C. K. Chen, K. H. Chen, T. J. Chuang, L. C. Chen and M. C. Lin, *J. Mater. Res.*, 1997, **12**, 322.
4 J. Martin-Gill, F. Martin-Gill, M. Sarlkaya, M. Quian, M. Jose-Yacaman and A. Rubio, *J. Appl. Phys.*, 1997, **81**, 2555.
5 K. Yamamoto, Y. Koga, K. Yase, S. Fijiara and M. Kubota, *Jpn. J. Appl. Phys., Part 2*, 1997, **36**, L230.
6 M. L. Cohen, *Solid State Commun.*, 1994, **45**, 92.
7 D. M. Teter, *MRS Bull.*, 1998, **23**, 22.
8 E. Knittle, R. M. Wentzcovitch, R. Jeanloz and M. L. Cohen, *Nature*, 1989, **337**, 349.
9 A. Y. Liu and R. M. Wentzcovitch, *Phys. Rev. B*, 1994, **50**, 10362.
10 J. Ortega and O. F. Sankey, *Phys. Rev. B*, 1995, **51**, 2624.
11 M. L. Cohen, *Int. J. Quantum Chem.*, 1997, **61**, 603.
12 D. M. Teter and R. J. Hemley, *Science*, 1996, **53**, 271.
13 M. Mattesini, S. F. Matar, A. Snis, J. Etourneau and A. Mavromaras, *J. Mater. Chem.*, 1999, **9**, 3151.
14 A. Y. Liu and M. L. Cohen, *Science*, 1989, **245**, 841.
15 J. V. Badding, *Adv. Mater.*, 1997, **11**, 877.
16 Y. Miyamoto, M. L. Cohen and S. G. Louie, *Solid State Commun.*, 1997, **102**, 605.
17 I. Alves, G. Demazeau, B. Tanguy and F. Weill, *Solid State Commun.*, 1999, **109**, 697.
18 W. Kohn and L. J. Sham, *Phys. Rev. A*, 1965, **140**, 1133; P. Hohenberg and W. Kohn, *Phys. Rev. B*, 1964, **136**, 864; D. M. Bylander and L. Kleinman, *Phys. Rev. B*, 1992, **46**, 13756; R. D. King-Smith, M. C. Payne and J. S. Lin, *Phys. Rev. B*, 1991, **44**, 13063; G. Kresse, Ph.D. thesis, Technische Universität Wien, 1993; N. D. Mermin, *Phys. Rev. A*, 1965, **137**, 1141; M. Weinert and J. W. Davenport, *Phys. Rev. B*, 1992, **45**, 13709; R. M. Wentzcovitch, J. L. Martins and P. B. Allen, *Phys. Rev. B*, 1991, **45**, 11372; A. de Vita and M. J. Gillan, *J. Phys. Condens. Matter*, 1991, **3**, 6225.
19 G. Kresse and J. Hafner, *Phys. Rev. B*, 1994, **49**, 14251.
20 G. Kresse and J. Hafner, *Phys. Rev. B*, 1993, **47**, 558.
21 G. Kresse and J. Furthmüller, *Comput. Mater. Sci.*, 1996, **6**, 15.
22 G. Kresse and J. Furthmüller, *Phys. Rev. B*, 1996, **54**, 11169.
23 D. Vanderbilt, *Phys. Rev. B*, 1990, **41**, 7892.
24 D. M. Ceperley and B. J. Alder, *Phys. Rev. Lett.*, 1980, **45**, 1196.
25 W. H. Press, B. P. Flannery, S. A. Teukolsky and W. T. Vetterling, *em Numerical Recipes*, Cambridge University Press, New York, 1986.
26 M. Methfessel and A. T. Paxton, *Phys. Rev. B*, 1989, **40**, 3616.
27 P. E. Blöchl, O. Jepsen and O. K. Anderson, *Phys. Rev. B*, 1994, **49**, 16223.
28 H. J. Monkhorst and J. D. Pack, *Phys. Rev. B*, 1976, **13**, 5188.
29 P. Blaha, K. Schwarz and J. Luitz, WIEN97, Vienna University of Technology, 1997, (Improved and updated UNIX version of the original copyrighted WIEN-code, P. Blaha, K. Schwarz, P. Sorantin and S. B. Trickey, *Comput. Phys. Commun.*, 1990, **59**, 399).
30 V. Eyert, *Electronic structure calculations for crystalline materials*, in: *Density Functional Methods: Applications in Chemistry and Materials Science*, ed. M. Sprungborg, Wiley, Chichester, 1997, pp. 233–304.
31 R. Hoffmann, *Angew. Chem., Int. Ed. Engl.*, 1987, **26**, 846.
32 A. Kokalj, *J. Mol. Graphics Modelling*, 2000, **18**, in press.

Paper a908903i